## Supplementary Data:

*ANU Argon Facility Technical Report: ANU11-2020*
*$^{40}Ar/^{39}Ar$ Analysis for National Argon Map*
*By Marnie Forster and Davood Vasegh*

## NAM Proposal 01:
## Filling the gaps: thermotectonic evolution of the east Tennant region and eastern Pine Creek Orogen

# Methods and procedures

## Sample selection and mineral separation:

Sample grains were provided by Geoscience Australia.

## Mineral details:

| Sample ID | Target Mineral | Mass (mg) | Grain Size (µm) |
|---|---|---|---|
| 2786115 (G01) | Muscovite | 5.1 | 250-420 |
| 2786115 (G02) | Biotite | 9.0 | 250-420 |
| 2786118 (G03) | Muscovite | 8.8 | 355-420 |
| 2786118 (G04) | Biotite | 7.1 | 355-420 |
| 2786131 (G05) | Biotite | 5.1 | 250-420 |
| 2799765 (G06) | Biotite | 6.5 | 250-420 |
| 2911541 (G08) | Biotite | 8.2 | 355-420 |
| AL08JHO165 (G09) | Biotite | 5.9 | 355-420 |
| AL08JHO165 (G10) | K-Feldspar | 6.3 | 355-420 |
| AL08LMG105 (G11) | Biotite | 8.7 | 355-420 |
| AL08LMG105 (G12) | Muscovite | 7.2 | 355-420 |
| AL08LMG105 (G13) | K-Feldspar | 7.8 | 355-420 |

Table 1: Mineral details

## Sample irradiation details:

Irradiation of samples for $^{40}Ar/^{39}Ar$ analysis was undertaken at the University of California Davis McClellan Nuclear Research Centre, CA, US in Central Facility position of TRIGA reactor without rotation, with 1.0mm of Cadmium shielding as ANU CAN #35 for 12.0 hours on 21-20, Dec 2019.

The calculated amounts of grains were weighed and recorded and then wrapped in labelled aluminium packets in preparation for irradiation. The sample filled foils were placed into a quartz irradiation canister together with aliquots of the flux monitor Biotite GA1550. The foil packets of GA1550 standards were dispersed 6-8mm apart throughout the irradiation canister, between the unknown age samples. In addition, packets containing $K_2SO_4$ and $CaF_2$ were placed in the middle of the canister to monitor argon isotope production from potassium and other interfering elements.

Irradiated samples were unwrapped upon their return to the Australian National University, and then rewrapped in tin foils in preparation for analysis under vacuum in the furnace. Tin foil is used because the melting temperature of tin is lower than the experiment starting point in the furnace and gasses from tin can be pumped away prior to the sample analysis.

# $^{40}Ar/^{39}Ar$ procedures and analysis information

## Methodology:

Temperature-controlled resistance furnace step-heating experiments is the technique that is used in the ANU Argon laboratory to extract argon isotopes from the samples to ensure 100% release of $^{39}Ar$. A sample is dropped into a cleaned furnace and heated to 400°C to melt the tin foil and then left in the furnace at 350°C for 8-12 hours to pump away unwanted gases. This cleaning procedure has proven to significantly improve the quality of the resultant data. The step-heating experiment then starts at 450°C, and each incremental heating step is heated at a constant temperature for 15 minutes. The heating process involves rapid heating to the setpoint temperature with no overshoot, then temperature is maintained for 15 minutes followed by rapid cooling; this procedure produces a square wave in temperature for each heating step. The heating step schedule for biotite and muscovite rises by 30°C increments (except for the last a few steps), with 30 steps per sample, while K-feldspar is analysed in more than 40 steps, including numerous isothermal steps. Diffusion experiments, as conducted in the ANU Argon laboratory, are designed to retrieve diffusion parameters which can be used in quantitative temperature-time modelling. The heating schedules are recorded in the XML tables for each sample.

Cleaning of the furnace between samples is vital in this method. The furnace is degassed four times at 1,450°C for 15 minutes and the gas pumped away prior to the loading of the subsequent sample. Blanks are measured to monitor the cleaning process. The flux monitor crystals are fused using a $CO_2$ continuous-wave laser. Gas released from either the flux monitors or each step of the sample analyses are exposed to three Zr-Al getters; two AP10 (Cold and hot) and one CP50, each for 10 minutes, to remove active gases. The purified extracted gasses are then isotopically analysed in the Argus VI mass spectrometer. The $^{40}Ar/^{39}Ar$ dating technique is adapted from McDougall and Harrison (1999) and described in Forster and Lister (2009).

Background levels are measured and subtracted from all analyses, from flux monitors and samples. The nuclear interfering values for the correction factors for the isotopes are listed below (Tetley et al 1980). These are measured for the reactions and uncertainties of $(^{36}Ar/^{37}Ar)_{Ca}$, $(^{39}Ar/^{37}Ar)_{Ca}$, $(^{40}Ar/^{39}Ar)_{K}$, $(^{38}Ar/^{39}Ar)_{K}$ and $(^{38}Ar)_{Cl}/(^{39}Ar)_{K}$, and were calculated prior to sample analyses.

## Mass spectrometer setup and procedures

Samples and standards were analysed in the Argon Laboratory at the Research School of Earth Science, The Australian National University, Canberra, Australia using a *Thermo Fisher ARGUS-VI* multi-collector mass spectrometer (Table 2).

| | |
|---|---|
| Mass Spectrometer: | Thermo Fisher Argus VI |
| Detector Type: | Faraday Cups only x5 |
| Calibrations: | 3 levels (Zero Offset, Gain and Cross Calibration) |
| Peak Centring: | Once for every measurement @H2 ($^{40}Ar$) |
| Measurement Cycles: | 51 cycles on all detectors |
| Extrapolation Method: | Exponential extrapolation and uncertainty |

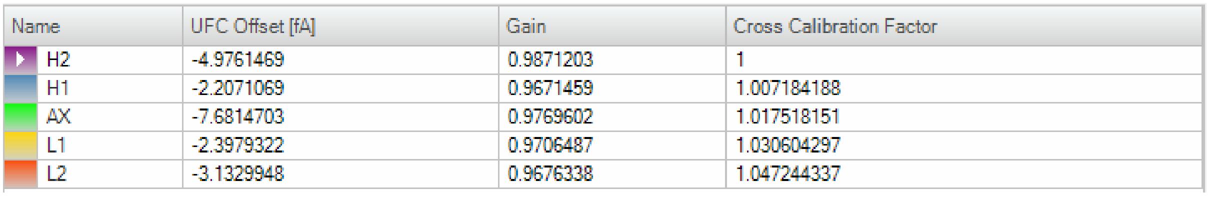

| Name | UFC Offset [fA] | Gain | Cross Calibration Factor |
|---|---|---|---|
| 🟪 H2 | -4.9761469 | 0.9871203 | 1 |
| 🟦 H1 | -2.2071069 | 0.9671459 | 1.007184188 |
| 🟩 AX | -7.6814703 | 0.9769602 | 1.017518151 |
| 🟨 L1 | -2.3979322 | 0.9706487 | 1.030604297 |
| 🟧 L2 | -3.1329948 | 0.9676338 | 1.047244337 |

Table 2: Detector Calibration Values

**The calculation parameters:**

| | |
|---|---|
| Lambda $^{40}$K (Renne et al 2011) | 5.5305E-10 |
| Lambda $^{37}$Ar (Kondev et al 2017) | 1.9798E-02 |
| Lambda $^{39}$Ar (Kondev et al 2017) | 7.0548E-06 |
| Lambda $^{36}$Cl (Kondev et al 2017) | 6.2985E-09 |
| Flux Monitor | GA1550 @ 99.18 ± 0.14 Ma |
| Total irradiation power | 12.00 MW |
| Irradiation Date | 20-21 Dec, 2019 |
| Irradiation shielding | Cadmium 1.0mm |

**Interfering isotope production ratios:**

| | |
|---|---|
| $(^{36}Ar/^{37}Ar)_{Ca}$ correction factor | 2.32216E-04 |
| $(^{39}Ar/^{37}Ar)_{Ca}$ correction factor | 6.16219E-04 |
| $(^{40}Ar/^{39}Ar)_{K}$ correction factor | 2.46117E-01 |
| $(^{38}Ar/^{39}Ar)_{K}$ correction factor | 1.16607E-02 |
| $(^{38}Ar)_{Cl}/(^{39}Ar)_{K}$ correction factor | 8.02854E-02 |
| Ca/K conversion factor | 1.90 |

**Atmospheric Argon correction ratio:**

| | |
|---|---|
| $^{40}Ar/^{36}Ar$ (Lee et al 2006) | 298.57 |
| $^{40}Ar/^{38}Ar$ (Lee et al 2006) | 1,583.52 |

**Representative air shot and blanks measurements:**

The discrimination factor was calculated by analysing five air shots on either side of sample analysis and is reported at 1amu. Table 3 shows an example of the analysed air shots and resultant calculation of discrimination factor.

| Date | $^{40}$Ar ± %err | | $^{38}$Ar ± %err | | $^{36}$Ar ± %err | | 1amu ± %err | | Reported Value |
|---|---|---|---|---|---|---|---|---|---|
| 18-Apr-2020 | 1,865.081 | 0.012 | 1.159 | 2.391 | 6.354 | 0.454 | 1.00426 | 0.233 | 1.0039643 ± 0.199% |
| 18-Apr-2020 | 1,863.083 | 0.013 | 1.214 | 3.303 | 6.309 | 0.586 | 1.00274 | 0.297 | |
| 18-Apr-2020 | 1,862.622 | 0.013 | 1.152 | 2.880 | 6.334 | 0.511 | 1.00379 | 0.261 | |
| 18-Apr-2020 | 1,863.052 | 0.011 | 1.205 | 2.846 | 6.351 | 0.624 | 1.00442 | 0.316 | |
| 18-Apr-2020 | 1,861.319 | 0.014 | 1.240 | 2.559 | 6.350 | 0.548 | 1.00461 | 0.279 | |

Table 3: Air Shots and Mass Discrimination Factor

The blank measurements are undertaken with different temperature schedules between 300°C and 1450°C, depending on the degassing behaviour and previous blank measurement results. The degassing and blank measurement procedure continues until the ratios of $^{40}$Ar, $^{38}$Ar and $^{36}$Ar drop to atmospheric ratios, and $^{39}$Ar and $^{37}$Ar drop below detectable levels. The entire procedure of degassing and blank measurements is repeated at the end of a set of samples. Blanks will be done in-between samples that belong to a set, with reduced steps at 300°C, 1300°C and 1450°C to check isotope levels. In addition, the mass of each sample is calculated so that the volume of gas released from each step overwhelms the volume of gas that may occur in the blank. Table 4 is a representative sequence of measured blank values recorded during a monitoring process.

| Temperature | $^{40}$Ar | $^{39}$Ar | $^{38}$Ar | $^{37}$Ar | $^{36}$Ar | $^{40}Ar/^{36}Ar$ |
|---|---|---|---|---|---|---|
| 300 | 1817.738 | 0.708661 | 1.209615 | ND* | 6.113996 | 297.3077 |
| 500 | 1879.391 | 0.741332 | 1.266375 | ND | 6.364901 | 295.2743 |
| 700 | 1911.306 | 0.759696 | 1.282523 | 0.095807 | 6.417252 | 297.8386 |
| 900 | 2053.27 | 0.775687 | 1.358664 | ND | 6.94095 | 295.8198 |
| 1100 | 2731.788 | 0.812587 | 1.788944 | 0.10454 | 9.192207 | 297.1852 |
| 1300 | 7305.089 | 1.038774 | 4.728446 | 0.139915 | 24.59727 | 296.9878 |

| | | | | | | |
|---|---|---|---|---|---|---|
| 1450 | 36811.09 | 2.436249 | 23.78145 | 0.23653 | 124.4077 | 295.8909 |
| 300 | 748.5261 | 0.344558 | 0.467985 | 0.019884 | 2.5069 | 298.5864 |
| 1300 | 1126.281 | 0.438838 | 0.704102 | 0.0207706 | 3.744338 | 300.7958 |
| 1450 | 2181.428 | 1.00614 | 1.377076 | 0.1028531 | 7.299197 | 298.8587 |

Table 4: Example of the blanks measurements during a sequence of blanks where isotopes were being monitored prior to sample analysis (* => Not Detectable). Temperature is °C.

## Data reduction software:

The calculations were done with an adapted version of *Noble* Software (2022, developed and adapted by the Australian National University Argon Laboratory) and all interpretations have been undertaken with *eArgon* (developed and adapted for ANU Argon Laboratory by G.S. Lister).

## Reported Data:

The reported data have been corrected for system backgrounds, mass discrimination, fluence gradients and atmospheric contamination. GA1550 standards were analysed, and an exponential best fit was then used for the calculation of the J-factor and J-factor uncertainty (Table 5).

Samples J-Factor, Mass Discrimination, and uncertainties:

| Sample Name | J-Factor ± %uncertainty | | Mass Discrimination Factor ± %uncertainty | | Measurement Date |
|---|---|---|---|---|---|
| 2786115 (G01) | 2.34272E-3 | 0.2317 | 1.0042435 | 0.179 | 25-Mar-2020 |
| 2786115 (G02) | 2.34246E-3 | 0.2317 | 1.0042435 | 0.179 | 26-Mar-2020 |
| 2786118 (G03) | 2.34224E-3 | 0.2317 | 1.0042435 | 0.179 | 28-Mar-2020 |
| 2786118 (G04) | 2.34199E-3 | 0.2317 | 1.0018961 | 0.321 | 07-Apr-2020 |
| 2786131 (G05) | 2.34173E-3 | 0.2317 | 1.0018961 | 0.321 | 08-Apr-2020 |
| 2799765 (G06) | 2.34151E-3 | 0.2317 | 1.0018961 | 0.321 | 10-Apr-2020 |
| 2911541 (G08) | 2.34108E-3 | 0.2317 | 1.0039643 | 0.199 | 12-Apr-2020 |
| AL08JHO165 (G09) | 2.34082E-3 | 0.2317 | 1.0039643 | 0.199 | 13-Apr-2020 |
| AL08JHO165 (G10) | 2.34060E-3 | 0.2317 | 1.0026306 | 0.247 | 23-Apr-2020 |
| AL08LMG105 (G11) | 2.34035E-3 | 0.2317 | 1.0026306 | 0.247 | 25-Apr-2020 |
| AL08LMG105 (G12) | 2.34009E-3 | 0.2317 | 1.0026306 | 0.247 | 26-Apr-2020 |
| AL08LMG105 (G13) | 2.33962E-3 | 0.2317 | 1.0026306 | 0.247 | 27-Apr-2020 |

Table 5: Sample analysis and calculation details

$^{40}$Ar/$^{39}$Ar isotopic data of the samples are supplied in the XML tables, which include details on the heating schedule, Argon isotopes abundances and their uncertainty levels, %Ar*, $^{40}$Ar*/$^{39}$Ar(K), Cumulative $^{39}$Ar%, calculated age and its uncertainty, Ca/K, Cl/K, J-Factor and its uncertainty. Noting that the reported uncertainties in the xml tables are at one sigma level and the fractional uncertainties are shown as % in the headings of the appropriate columns of data tables. The components involved in the calculation of the uncertainties are listed in Table 6.

| Uncertainty of: | Components involved in the calculation |
|---|---|
| Isotope Abundances | Uncertainty of isotope measurement<br>Uncertainty of Mass Discrimination Factor (except for $^{39}$Ar) |
| J-Factor | Uncertainty of $^{40}$K Decay Constant<br>Uncertainty of Age of the Flux monitor<br>Uncertainty of Flux monitor isotopes abundances |

| | |
|---|---|
| Calculated Age | Uncertainty of Isotopes Abundances<br>J-Factor value and uncertainty of J-Factor<br>$^{40}$K Decay Constant value and uncertainty of $^{40}$K Decay Constant |

Table 6: Components involved in the calculation of each uncertainty.

## References:

Forster, M.A. and Lister, G.S. 2004. The interpretation of 40Ar/39Ar apparent age spectra produced by mixing: application of the method of asymptotes and limits. Journal of Structural Geology 26, 287–305

Forster, M.A. and Lister, G.S. 2009. Core-complex-related extension of the Aegean lithosphere initiated at the Eocene-Oligocene transition. Journal Geophysical Research, 114, B02401.

Kondev, F.G. and Naimi, S. 2017. The NUBASE2016 evaluation of nuclear properties. Chinese physics C, 41(3), p.030001.

Lee, J.Y., Marti, K., Severinghaus, J.P., Kawamura, K., Yoo, H.S., Lee, J.B. and Kim, J.S. 2006. A redetermination of the isotopic abundances of atmospheric Ar. Geochimica et Cosmochimica Acta, 70(17), 4507-4512.

McDougall, I. and Harrison, T.M. (Eds.). 1999. Geochronology and Thermochronology by the 40Ar/39Ar Method, 2nd ed., 269 pp. Oxford Univ. Press, New York.

Renne, P.R., Balco, G., Ludwig, K.R., Mundil, R. and Min, K., 2011. Response to the comment by WH Schwarz et al. on “Joint determination of 40K decay constants and 40Ar∗/40K for the Fish Canyon sanidine standard, and improved accuracy for 40Ar/39Ar geochronology” by PR Renne et al. (2010). Geochimica et Cosmochimica Acta, 75(17), pp.5097-5100.

Spell, T. L. and I. McDougall. 2003. Characterization and calibration of 40Ar/39Ar dating standards. Chemical Geology, 198, 189–211.

Tetley, N., McDougall, I. & Heydegger, H.R. 1980. Thermal neutron interferences in the 40Ar/39Ar dating technique. Journal Geophysical Research, 85, 7201–7205.